Theory of intersubband cyclotron combined resonances in the silicon space-charge layer

T. Ando*
IBM Thomas J. Watson Research Center, Yorktown Heights, New York 10598
(Received 15 September 1978)

The subband structure and the intersubband optical-absorption spectrum are calculated in n-channel inversion and accumulation layers on the Si (100) surface in magnetic fields tilted from the direction normal to the surface. An approximation scheme based on the local-density-functional theory is employed. Effects of magnetic fields on the exchange-correlation potential are completely neglected. Combined intersubband-cyclotron transitions between different Landau levels associated with the ground and excited subbands are allowed in addition to the main transition between the same Landau levels. When the amplitudes of the combined resonances are sufficiently small, they are not affected by the depolarization effect, while the main transition is fully influenced and its position is shifted from the corresponding subband energy separation. This is shown to be also true of accumulation layers, where the subband structure is very complicated because higher quasicontinuum subbands lie close to the ground and the first excited subband. The agreement between the theory and recent experiments of Beinvogl and Koch is satisfactory concerning relative positions of the main and combined transitions in accumulation layers. This indicates that our calculations of both the depolarization effect and the subband energy separations are essentially correct. There remain disagreements especially concerning amplitudes of the combined resonances.

I. INTRODUCTION

When a strong electric field is applied normal to a semiconductor surface, the electron motion in the z direction, the direction perpendicular to the surface, is quantized and the two-dimensional electric subbands are formed. The structure of the subbands is determined self-consistently, since the effective potential which gives subband energy levels and wave functions is in turn a functional of the electron density distribution. The so-called self-consistent Hartree approximation combined with the effective-mass approximation, proposed by Stern and Howard,[1] has been used for subband structure calculations and turned out to be successful in a number of systems.[2] In inversion and accumulation layers on silicon surfaces, however, the Hartree approximation in known to be insufficient and many-body effects such as exchange and correlation strongly modify the subband structure.[3-6] The intersubband optical absorption is the ideal way of studying such subband structure, and has been observed in various systems by different people.[7-10] However, the optical absorption is known to be affected by the depolarization effect and its local-field correction, and the resonance energy is shifted from the subband energy separation.[11-13] A previous calculation of the optical spectrum in n-channel layers on the Si (100) surface has given results which are in good agreement with experiments.[4] A direct comparison of the subband structure itself has not been possible since the strength of the depolarization effect is still unknown experimentally. In a previous paper,[14] the optical spectrum in the presence of magnetic fields tilted from the normal to the surface was theoretically studied in an inversion layer and was suggested to determine subband energy separations and resonance energies independently. Effects of magnetic fields on the subband structure were completely neglected and treated as a small perturbation. In this paper we calculate the subband structure and optical spectrum without any such restrictions and show that independent determination is possible also in accumulation layers.

The effects of a magnetic field is one of the best ways to study the details of the subband structure and the above additional corrections. When a magnetic field is applied in the y direction parallel to the surface, electrons moving in the positive and negative x directions are affected by different Lorentz forces and the subband structure is modified.[15-17] The intersubband optical-absorption spectrum is also influenced by the field. Usually, for the ground subband the radius of the cyclotron motion (typically, 81 Å in 100 kOe) is much larger than the spread of the wave function $(\langle z^2\rangle - \langle z\rangle^2)^{1/2}$ (~15 Å, typically), and the magnetic field can be treated as a small perturbation. As for excited subbands especially in the accumulation layer, this is no longer true and the states become a mixture of electric subbands and magnetic surface states.[16] The magnetic-field effect on the absorption spectrum is very sensitive to the degree of binding, especially of excited subbands. Beinvogl *et al.* observed broadening of the line shape and a shift of the peak energy in n-channel layers on the Si (100) surface.[18] A corresponding theoretical calculation of the effect of the magnetic field gave

results which were in good agreement with the experiments.[19] This supports the calculated subband structure in the absence of a magnetic field, although indirectly.

When a magnetic field is applied in the z direction, each subband is further quantized into discrete Landau levels. The singular nature of the density of states, especially in extremely strong magnetic fields ($\gtrsim$100 kOe), can cause an important modification of the many-body effects similar to the enhancement of the spin splitting,[20] and might modify the subband structure. But there has been no theoretical and experimental work on this problem. The singular density of states has been shown to cause a new kind of quantum oscillation in the line shape of the intersubband absorption.[21]

In magnetic fields tilted from the z direction, the perpendicular and parallel motions of electrons are coupled and the combined intersubband-cyclotron transitions (transitions between different Landau levels of ground and excited subbands) become allowed. Such combined resonance has first been observed in a system of electrons trapped outside of liquid helium by the image potential. Zipfel *et al.* observed a pair of satellite peaks, displaced symmetrically by about the Landau-level separation from the main intersubband transition.[22] In inversion and accumulation layers the existence of the depolarization effect makes the spectrum much more complicated, but the observation of the combined resonances can provide important information on the strength of the depolarization effect.[14] The purpose of the present paper is to present results of a calculation of the subband structure and the optical spectrum in n-channel layers on the Si (100) surface in such tilted magnetic fields.

We employ an approximation scheme based on the density-functional formulation of Hohenberg, Kohn, and Sham.[23-25] We use a local exchange-correlation potential calculated previously[4] for both the density distribution and the subband energy levels. The energy dependence of the exchange-correlation potential is very small and can be neglected, as has been shown previously.[4] We use the same form of the exchange-correlation potential even for the calculation of the response to dynamical external electric fields. Although this approximation is not justified from rigorous theoretical grounds, it is expected to give a reasonable order of magnitude of the local-field correction to the depolarization effect.[13,26] Further, effects of magnetic fields on the exchange-correlation potential are completely neglected, which is expected to work well in parallel magnetic fields but might cause some errors in extremely strong perpendicular fields. In the present case where the perpendicular magnetic component is not so strong, the level quantization effect on many-body effects is still not appreciable and this approximation does not give rise to serious errors. In Sec. II we briefly discuss the method of calculating the subband structure and the optical spectrum in tilted magnetic fields. Numerical results and discussions of them are given in Sec. III, and Sec. IV is used for summary and conclusion.

II. SUBBAND STRUCTURE AND INTERSUBBAND ABSORPTION SPECTRUM

Calculation of the subband structure and the optical spectrum is straightforward in the present approximation and proceeds essentially in the same way as described in a previous paper.[13] The subband structure can be calculated by solving the Schrödinger equation,

$$\mathcal{H}\psi(x,y,z)=E\psi(x,y,z)\,, \tag{2.1}$$

with

$$\mathcal{H}=\frac{1}{2m_t}\left(p_x+\frac{e}{c}H_y z\right)^2+\frac{1}{2m_l}\left(p_y+\frac{e}{c}H_z x\right)^2 + \frac{1}{2m_l}p_z^2+V_{\rm eff}(z)\,, \tag{2.2}$$

where m_l and m_t are the effective masses in the z direction, the direction normal to the surface, and in the x-y plane (the surface), respectively, the magnetic field $(0,H_y,H_z)$ is assumed to be applied in the y-z plane, and

$$V_{\rm eff}(z)=v_{\rm depl}(z)+v_{\rm image}(z)+v_H(z)+v_{\rm xc}(n(z);z)\,. \tag{2.3}$$

Here we have

$$v_{\rm depl}(z)\cong(4\pi e^2/\kappa_{\rm Si})N_{\rm depl}z\,, \tag{2.4}$$

$$v_{\rm image}(z)=(\kappa_{\rm Si}-\kappa_{\rm ox})e^2/4\kappa_{\rm Si}(\kappa_{\rm Si}+\kappa_{\rm ox})z\,, \tag{2.5}$$

and

$$v_H(z)=\frac{4\pi e^2}{\kappa_{\rm Si}}N_s z-\frac{4\pi e^2}{\kappa_{\rm Si}}\int_0^z dz'\int_0^{z'}dz''\,n(z'')\,, \tag{2.6}$$

where $\kappa_{\rm Si}$ and $\kappa_{\rm ox}$ are the static dielectric constants of Si and SiO_2, respectively, $n(z)$ is the density distribution of electrons in the inversion or accumultation layer, N_s is the electron concentration in a unit area, and $N_{\rm depl}$ is the concentration of the fixed negative space charges in a unit area. The exchange-correlation potential $v_{\rm xc}(n(z);z)$ becomes dependent explicitly on z because of the image effect.[4] We have simply replaced the potential due to $N_{\rm depl}$ by a triangular potential and neglected the difference between the accumulation layer and the

inversion layer on extremely-low-doped silicon (called quasiaccumulation), which is usually justified since the thickness of the region where the band is bent down is much larger than that of the inversion and accumulation layer.

To solve (2.1) we separate the Hamiltonian into

$$\mathcal{H}=\mathcal{H}_{\perp}+\mathcal{H}_{\parallel}+\mathcal{H}', \tag{2.7}$$

with

$$\mathcal{H}_{\perp}=\frac{1}{2m_l}p_z^2+V_{\text{eff}}(z)+\frac{\hbar^2}{2m_t}\frac{z^2}{l_{\parallel}^4}, \tag{2.8}$$

$$\mathcal{H}_{\parallel}=\frac{1}{2m_t}p_x^2+\frac{1}{2m_t}\left(p_y+\frac{e}{c}H_z x\right)^2, \tag{2.9}$$

and

$$\mathcal{H}'=(\hbar/m_t)(zp_x/l_{\parallel}^2), \tag{2.10}$$

where $l_{\parallel}^2=c\hbar/eH_y$ and $l_{\perp}^2=c\hbar/eH_z$. As the basis we choose

$$\psi_{nNX}(x,y,z)=L^{-1/2}\exp\left(-i\frac{Xy}{l_{\perp}^2}-i\frac{z_{nn}}{l_{\parallel}^2}(x-X)\right)\times\chi_N(x-X)\zeta_n(z), \tag{2.11}$$

with

$$\chi_N(x)=i^N(2^N N!\pi^{1/2}l_{\perp})^{-1/2}H_N\left(\frac{x}{l_{\perp}}\right)\exp\left(-\frac{x^2}{2l_{\perp}^2}\right), \tag{2.12}$$

and

$$z_{nm}=\int_0^{\infty}dz\,\zeta_n(z)z\zeta_m(z), \tag{2.13}$$

where L^2 is the area of the system, X is a center coordinate, and $H_N(x)$ is the Hermite polynomial. $\zeta_n(z)$ is chosen to be real and satisfies

$$\mathcal{H}_{\perp}\zeta_n(z)=E_n(H_y)\zeta_n(z). \tag{2.14}$$

It is clear that (2.11) constitutes a complete orthonormal set. The matrix elements of the Hamiltonian can straightforwardly be calculated and are given by

$$(n'N'X'|\mathcal{H}|nNX)=\delta_{XX'}\Big[\Big(E_n-\frac{\hbar^2}{2m_l}\frac{z_{nn}^2}{l_{\parallel}^4}+(N+\tfrac{1}{2})\hbar\omega_c\Big)\delta_{nn'}\delta_{NN'}+(1-\delta_{nn'})(n'N'|\mathcal{H}'|nN)\Big], \tag{2.15}$$

with $\omega_c=eH_z/m_tc$. Here one has defined

$$(n'N'|\mathcal{H}'|nN)=\frac{\hbar^2}{2m_t}\frac{z_{n'n}}{l_{\parallel}^2l_{\perp}}\Big[\Big(\frac{N+1}{2}\Big)^{1/2}J_{N'N+1}(\Delta_{n'n})+\Big(\frac{N'+1}{2}\Big)^{1/2}J_{NN'+1}(\Delta_{n'n})+\Big(\frac{N}{2}\Big)^{1/2}J_{N'N-1}(\Delta_{n'n})+\Big(\frac{N'}{2}\Big)^{1/2}J_{NN'-1}(\Delta_{n'n})-\frac{l_{\perp}}{l_{\parallel}^2}(z_{nn}+z_{n'n'})J_{N'N}(\Delta_{n'n})\Big], \tag{2.16}$$

with

$$\Delta_{n'n}=(l_{\perp}/l_{\parallel}^2)(z_{n'n'}-z_{nn}), \tag{2.17}$$

and

$$J_{NN'}(x)=J_{N'N}(-x)=\left(\frac{N'!}{N}\right)^{1/2}\left(\frac{x}{2^{1/2}}\right)^{N-N'}L_{N'}^{N-N'}(\tfrac{1}{2}x^2)\exp(-\tfrac{1}{4}x^2), \tag{2.18}$$

where $L_N^{\alpha}(x)$ is the associated Laguerre polynomial. We have used the result

$$\int dx\,\chi_N^*(x)\chi_{N'}(x)\exp(iq_xx)=J_{NN'}(l_{\perp}q_x). \tag{2.19}$$

The above choice of the basis is convenient since the Hamiltonian is diagonal with respect to the motion in the x-y plane if we can neglect couplings between different subbands. The energy spectrum can be calculated by diagonalizing the large real symmetric matrix (2.15). We define the matrix S which makes the Hamiltonian diagonal, i.e.,

$$\psi_{\mu X}(x,y,z)=\sum_{nN}\psi_{nNX}(x,y,z)S_{nN,\mu}, \tag{2.20}$$

with

$$(S^{-1}\mathcal{H}S)_{\mu\nu}=E_{\mu}\delta_{\mu\nu}. \tag{2.21}$$

The density distribution becomes

$$n(z)=\frac{g_Sg_v}{2\pi l_{\perp}^2}\sum_{\mu}f(E_{\mu})\rho_{\mu\mu}(z), \tag{2.22}$$

with

$$\rho_{\mu\nu}(z)=\rho_{\nu\mu}(z)=\frac{2\pi l_{\perp}^2}{L^2}\sum_X\psi_{\mu X}^*(x,y,z)\psi_{\nu X}(x,y,z)=\sum_{n'N'}\sum_{nN}\zeta_{n'}(z)S_{n'N',\mu}J_{N'N}(\Delta_{n'n})S_{nN,\nu}\zeta_n(z), \tag{2.23}$$

where $f(\varepsilon)$ is the Fermi distribution function and satisfies

$$N_s = g_s g_v \frac{1}{2\pi l_\perp^2} \sum_\mu f(E_\mu) . \tag{2.24}$$

We have neglected the spin and valley splittings and assumed the degeneracy g_s and g_v, which is expected to give rise to no serious errors.

Let $\Delta n(z)\exp(-i\omega t)$ be the change in the electron density distribution due to an external electric field D in the z direction. The change in the effective potential becomes

$$\mathcal{H}_1 \exp(-i\omega t) = [eDz + \Delta v_H(z) + \Delta v_{xc}(z)\exp(-i\omega t) , \tag{2.25}$$

with

$$\Delta v_H(z) = -\frac{4\pi e^2}{\kappa_{Si}} \int_0^z dz' \int_0^{z'} dz'' \, \Delta n(z'') , \tag{2.26}$$

and

$$\Delta v_{xc}(z) = \frac{\partial v_{xc}(z)}{\partial n(z)} \Delta n(z) . \tag{2.27}$$

The last two terms on the right-hand side of (2.25) describe the depolarization effect and its local-field correction. Using the linear response theory of Kubo,[27] we can calculate the induced density in the presence of the perturbation.

$$\begin{aligned}\Delta n(z) &= g_v g_s \frac{1}{L^2} \sum_{\mu X} \sum_{\nu X'} [f(E_\nu) - f(E_\mu)] \\ &\quad \times \frac{(\mu X|\mathcal{H}_1|\nu X')}{\hbar\omega - E_\nu + E_\mu} \psi^*_{\mu X} \psi_{\nu X'} \\ &= 2 \frac{g_v g_s}{2\pi l_\perp^2} \sum_\mu \sum_\nu f(E_\nu)[1 - f(E_\mu)] \\ &\quad \times \frac{E_{\mu\nu}(\mu|\mathcal{H}_1|\nu)}{(\hbar\omega)^2 - E_{\mu\nu}^2} \rho_{\mu\nu}(z) ,\end{aligned} \tag{2.28}$$

with $E_{\mu\nu} = E_\mu - E_\nu$, where we have used the fact that the matrix element of the perturbation is diagonal with respect to X and independent of X. Substitution of (2.28) into (2.25) gives a self-consistency equation which determines $\Delta n(z)$. Let us define

$$\begin{aligned}u_{(\mu\nu)} &= (eD)^{-1} \left(\frac{2m_1}{\hbar^2} E_{\mu\nu}\right)^{-1/2} \frac{(\mu|\mathcal{H}_1|\nu)}{E_{\mu\nu}^2 - (\hbar\omega)^2} \\ &\quad \times \{f(E_\nu)[1 - f(E_\mu)]\}^{1/2} ,\end{aligned} \tag{2.29}$$

and

$$\begin{aligned}\Lambda_{(\mu\nu)(\mu'\nu')} &= [E_{\mu\nu}^2 - (\hbar\omega)^2]\delta_{\mu\mu'}\delta_{\nu\nu'} + \frac{g_v g_s}{2\pi l_\perp^2 N_s} \\ &\quad \times \{f(E_\nu)[1 - f(E_\mu)]\}^{1/2} E_{\mu\nu} (\alpha_{(\mu\nu)(\mu'\nu')} - \beta_{(\mu\nu)(\mu'\nu')}) E_{\mu'\nu'} \{f(E_{\nu'})[1 - f(E_{\mu'})]\}^{1/2} ,\end{aligned} \tag{2.30}$$

with

$$\alpha_{(\mu\nu)(\mu'\nu')} = 2N_s \frac{4\pi e^2}{\kappa_{Si}} (E_{\mu\nu} E_{\mu'\nu'})^{-1/2} \int_0^\infty dz \, \rho_{\mu\nu}(z) \int_0^z dz' \int_0^{z'} dz'' \, \rho_{\mu'\nu'}(z'') , \tag{2.31}$$

and

$$\beta_{(\mu\nu)(\mu'\nu')} = -2N_s (E_{\mu\nu} E_{\mu'\nu'})^{-1/2} \int_0^\infty dz \, \rho_{\mu\nu}(z) \frac{\partial v_{xc}}{\partial n(z)} \rho_{\mu'\nu'}(z) . \tag{2.32}$$

We have

$$\begin{aligned}&\sum_{\mu'} \sum_{\nu'} \Lambda_{(\mu\nu)(\mu'\nu')} u_{\mu'\nu'} \\ &\quad = \left(\frac{2m_1}{\hbar^2} E_{\mu\nu}\right)^{1/2} z_{\mu\nu} \{f(E_\nu)[1 - f(E_\mu)]\}^{1/2} .\end{aligned} \tag{2.33}$$

The induced current in the z direction is given by

$$j(z)\exp(-i\omega t) = -(-i\omega)(-e) \int_0^z dz' \, \Delta n(z') \exp(-i\omega t) . \tag{2.34}$$

The electric field becomes

$$E(z) = D - (4\pi i/\omega\kappa_{Si}) j(z) . \tag{2.35}$$

Thus the absorption in a unit area is

$$P = \tfrac{1}{2} \mathrm{Re} \int_0^\infty dz \, j(z) E^*(z) = \tfrac{1}{2} \mathrm{Re} \tilde{\sigma}_{zz}(\omega) D^2 , \tag{2.36}$$

where

$$\begin{aligned}\tilde{\sigma}_{zz}(\omega) &= \frac{1}{D} \int_0^\infty dz \, j(z) \\ &= N_s e^2 (-i\omega) \frac{\hbar^2}{m_1} \frac{g_v g_s}{2\pi l_\perp^2 N_s} \\ &\quad \times \sum_\mu \sum_\nu \sum_{\mu'} \sum_{\nu'} u_{(\mu\nu)} \Lambda_{(\mu\nu)(\mu'\nu')} u_{(\mu'\nu')} .\end{aligned} \tag{2.37}$$

If we introduce a matrix U which diagonalizes Λ, i.e.,

$$\sum_\mu \sum_\nu \sum_{\mu'} \sum_{\nu'} \Lambda_{(\mu\nu)(\mu'\nu')} U_{(\mu\nu),\eta} U_{(\mu'\nu'),\eta'} = E_\eta^2 \delta_{\eta\eta'} , \tag{2.38}$$

we have

$$\tilde{\sigma}_{zz}(\omega) = N_s e^2 (-i\omega) \frac{\hbar^2}{m_1} \sum_\eta \frac{f_\eta}{E_\eta^2 - (\hbar\omega)^2 - 2i\hbar\omega(\hbar/\tau)} , \tag{2.39}$$

with

$$f_\eta = \frac{g_v g_s}{2\pi l_\perp^2 N_s}\left[\sum_\mu\sum_\nu\left(\frac{2m_l}{\hbar^2}E_{\mu\nu}\right)^{1/2} \times z_{\mu\nu}\{f(E_\nu)[1-f(E_\mu)]\}^{1/2}U_{(\mu\nu),\eta}\right]^2 . \tag{2.40}$$

It is easy to show that

$$\sum_\eta f_\eta = 1 . \tag{2.41}$$

We have introduced a phenomenological constant relaxation time τ for the calculation of the absorption line shape and neglected various problems on the broadening like a quantum oscillation[21] and a motional narrowing effect.[28] This is sufficient to see the qualitative behavior of the line shape.

Consider the case that the magnetic field and consequently mixing between different subbands are sufficiently small. This is usually the case in inversion layers with large N_{depl}. We have

$$E_\mu = E_{nN} = E_n(H_y) + (N+\tfrac{1}{2})\hbar\omega_c - \frac{\hbar^2}{2m_t}\frac{z_{nn}^2}{l_\parallel^4}$$

$$\cong E_n + (N+\tfrac{1}{2})\hbar\omega_c + \frac{\hbar^2}{2m_t}\frac{1}{l_\parallel^4}[(z^2)_{nn} - (z_{nn})^2] , \tag{2.42}$$

$$\rho_{nN,n'N'}(z) = J_{NN'}(\Delta_{nn'})\xi_n(z)\xi_{n'}(z) , \tag{2.43}$$

and

$$z_{nN,n'N'} = J_{NN'}(\Delta_{nn'})z_{nn'} , \tag{2.44}$$

where E_n is the energy of the bottom of the subband and z_{nn} and $(z^2)_{nn}$ are the corresponding matrix elements in the absence of a magnetic field. The level structure is schematically illustrated in Fig. 1. In the presence of H_y the electron dispersion relation is shifted in the k_x direction by $-z_{nn}/l_\parallel^2$ in addition to a diamagnetic shift $(\hbar^2/2m_t)[(z^2)_{nn}-(z_{nn})^2]/l_\parallel^4$. Those shifts are larger for higher subbands, since they are more weakly bound. We assume further that the energy $\hbar\omega$ of the incident far-infrared light is close to $E_{n0}=E_n - E_0$ and neglect contributions of transitions to other subbands to the change in the density distribution. We can neglect $\hbar\omega_c$ in comparison with E_{n0} except in the first term of the right-hand side of (2.30). We have

$$\alpha_{(nN_1,0N_1')(nN_2,0N_2')} - \beta_{(nN_1,0N_1')(nN_2,0N_2')} = J_{N_1N_1'}(\Delta_{n0})J_{N_2N_2'}(\Delta_{n0})(\alpha_{nn}-\beta_{nn}) = J_{N_1N_1'}(\Delta_{n0})J_{N_2N_2'}(\Delta_{n0})\gamma_{nn} , \tag{2.45}$$

where α_{nn}, β_{nn}, and γ_{nn} are the corresponding quantities in the absence of a magnetic field. We can easily solve (2.33) and get

$$\tilde{\sigma}_{zz}(\omega) = \frac{N_s e^2 f_{n0}}{m_l}\frac{(-i\hbar^2\omega)}{E_{n0}^2}L_n(\omega)[1+\gamma_{nn}L_n(\omega)]^{-1} , \tag{2.46}$$

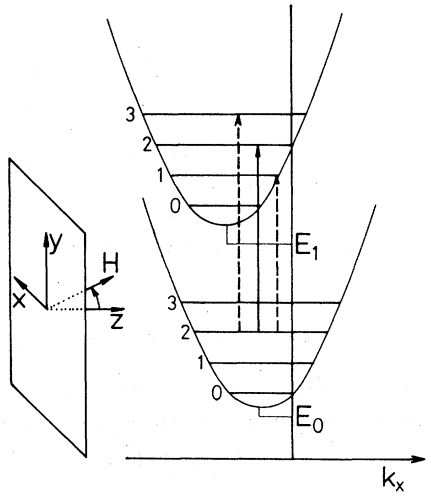

FIG. 1. Schematic illustration of the subband and Landau-level structure in an inversion layer in a tilted magnetic field. The magnetic field is in the y-z plane, where the z direction has been chosen in the direction normal to the surface. The two parabolas represent the dispersion relation in the absence of H_z. Because of shifts of the center of the Landau orbit in k_x-k_y space, combined intersubband-cyclotron transitions become allowed in addition to the main transition.

with $f_{n0} = 2m_l z_{n0}^2 E_{n0}/\hbar^2$ being the oscillator strength for the transition $0\to n$ in the absence of a magnetic field and

$$L_n(\omega) = \frac{g_v g_s}{2\pi l_\perp^2 N_s}\sum_N\sum_{N'} f(E_{0N'})[1-f(E_{nN})] \times \frac{E_{n0}^2 J_{NN'}(\Delta_{n0})^2}{(E_{nN}-E_{0N'})^2 - (\hbar\omega)^2 - 2i\hbar\omega(\hbar/\tau)} . \tag{2.47}$$

This is the same as the expression obtained previously.[14] It shows that the intensity of the transition $0N'\to nN$ is proportional to $J_{NN'}(\Delta_{n0})^2$, which is essentially the square of the overlapping integral of cyclotron orbits displaced from each other by $(z_{nn}-z_{00})/l_\parallel^2$ in the k_x-k_y space. This is easily understood from Fig. 1. When $\Delta_{n0}\ll 1$, we get[29]

$$J_{NN}(\Delta_{n0})^2 \cong 1 - \frac{2N+1}{2}\Delta_{n0}^2 = 1 - (N+\tfrac{1}{2})\frac{l_\perp^2(z_{nn}-z_{00})^2}{l_\parallel^4} , \tag{2.48}$$

and

$$J_{NN\pm1}(\Delta_{n0})^2 \cong \tfrac{1}{2}(N+\tfrac{1}{2}\pm\tfrac{1}{2})\frac{l_\perp^2(z_{nn}-z_{00})^2}{l_\parallel^4} . \tag{2.49}$$

Thus the effect of H_y is larger for higher Landau levels and the combined resonance for $\Delta N=+1$ $(0N\to nN+1)$ is larger than that for $\Delta N=-1$. Further it is clear that the position of the combined resonances $\Delta N\neq 0$ is given by $E_{n0}+\Delta N\hbar\omega_c$ when the amplitude is sufficiently small, while the

main resonance is determined by $\tilde{E}_{n0}=(1+\gamma_{nn})^{1/2}E_{n0}$. Thus we can determine the strength of the depolarization effect γ_{nn} from the relative shift of the combined and main resonances in such a case. When $H_y \gg H_z$, on the other hand, the line shape becomes an elliptic form except for the appearance of the quantum structure caused by the nonzero H_z. Such a behavior of the resonance line shape has been theoretically demonstrated in a previous paper.[14]

III. RESULTS AND DISCUSSION

In the following numerical calculation we use $m_t=0.1905m$, $m_l=0.916m$, $\kappa_{Si}=11.9$, $\kappa_{ox}=3.9$, and $g_v=g_s=2$, where m is the free-electron mass. We take into account 5 subbands ($n=0$–4) and 20 Landau levels ($N=0$–19) for the inversion case, and 15 subbands ($n=0$–14) and 20 Landau levels for the accumulation case in the calculation of energy levels. As for the calculation of the optical spectrum we include 40 lowest excited levels ($\mu=\mu_F\sim\mu_F+39$, where μ_F denotes the index of the level at which the Fermi level lies). Those numbers, which are limited by the computational time, might not be sufficient for higher levels especially in accumulation layers, depending on the strength of the magnetic field. They are of course not enough to reproduce the total level structure of the quasicontinuum states in accumulation layers, but are expected to be reasonable for the discussion of the optical transition from the ground subband.

Figure 2 gives transition energies and corresponding oscillator strengths, and the optical spectrum given by $\mathrm{Re}\tilde{\sigma}_{zz}(\omega)$ for several different amounts of the broadening $\hbar/\tau$ in an inversion layer for $N_s=2\times10^{12}$ cm^{-2}, $N_{\mathrm{depl}}=1\times10^{11}$ cm^{-2}, and $H_y=H_z=50$ kOe. The Landau-level separation $\hbar\omega_c$ is 3.04 meV, and in the absence of a magnetic field we have $\gamma_{11}\sim0.2$, $E_{10}\sim28$ meV, and $\Delta_{10}\sim0.27$. The Fermi level lies in the Landau level $N=4$ of the ground subband. A large transition at $\hbar\omega\sim27.4$ meV is identified as the main resonance ($\Delta N=0$) from the ground to the first excited subband. We can see corresponding combined resonances for $\Delta N=-1$ around $\hbar\omega\sim22.6$ meV, for $\Delta N=+1$ around $\hbar\omega\sim29$ meV, and for $\Delta N=+2$ around $\hbar\omega\sim31.8$ meV. The main resonance is clearly shifted relatively from the midpoint of the positions of the combined resonances because of the depolarization effect. Since the amplitude of the combined resonance $\Delta N=+1$ is already quite large, its position is also shifted although slightly and the shift of the main transition is smaller than in the absence of a magnetic field. The amplitudes of the combined resonances are roughly given by the perturbation results (2.49), but the depolarization effect (positive γ_{11}) has enhanced the strength of the combined resonance $\Delta N=+1$. Absorptions at $\hbar\omega\sim37.8$ meV are the main transition to the second excited subband, and transitions at $\hbar\omega\sim34.5$ meV and $\hbar\omega\sim41$ meV are corresponding combined resonances ($\Delta N=\pm1$), which are located at an almost equal distance from the main resonance. We can also see transitions to the third excited subband at $\hbar\omega\sim45$ meV and combined resonances at $\hbar\omega\sim42$ meV and $\hbar\omega\sim48$ meV.

Figure 3 gives the optical spectrum for $H_y=150$ kOe. Other parameters are the same as in Fig. 2.

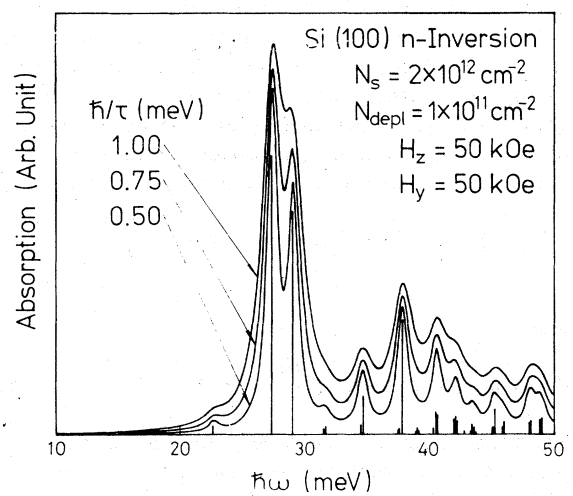

FIG. 2. Calculated optical-absorption spectrum in an n-channel inversion layer on the Si (100) surface in a tilted magnetic field. $N_s=2\times10^{12}$ cm^{-2}, $N_{\mathrm{depl}}=1\times10^{11}$ cm^{-2}, $H_z=50$ kOe, and $H_y=50$ kOe.

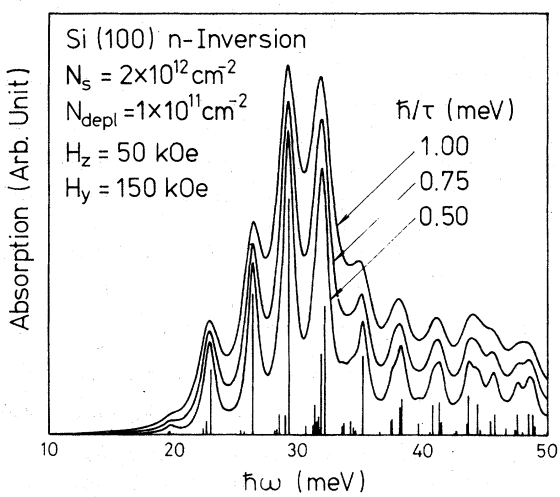

FIG. 3. Optical-absorption spectrum in an n-channel inversion layer on the Si (100) surface in a tilted magnetic field. $N_s=2\times10^{12}$ cm^{-2}, $N_{\mathrm{depl}}=1\times10^{11}$ cm^{-2}, $H_z=50$ kOe, and $H_y=150$ kOe.

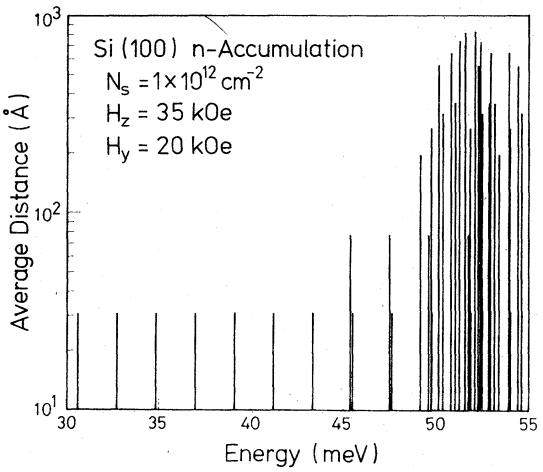

FIG. 4. Average values of z as a function of energies of low-lying levels in an n-channel accumulation layer on the Si (100) surface in a tilted magnetic field. $N_s = 1\times10^{12}$ cm^{-2}, $H_z = 35$ kOe, and $H_y = 20$ kOe.

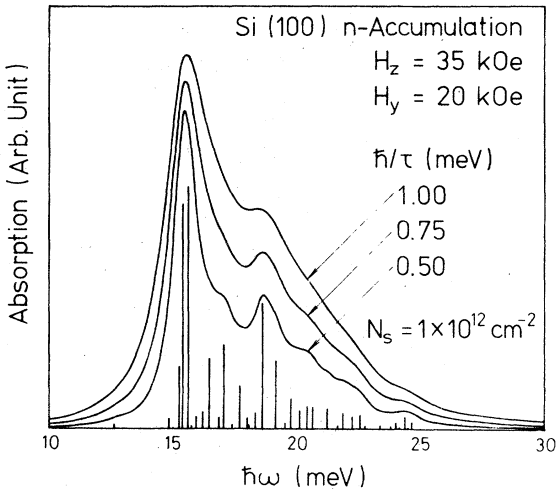

FIG. 5. Calculated optical spectrum in an n-channel accumulation layer on the Si (100) surface in a tilted magnetic field. $N_s = 1\times10^{12}$ cm^{-2}, $H_z = 35$ kOe, and $H_y = 20$ kOe.

Mixing between different subbands is now appreciable especially for excited subbands. There is no essential difference of main and combined resonances and the overall line shape below $\hbar\omega \sim 35$ meV becomes close to that in a parallel magnetic field except for the appearance of many peaks due to nonzero H_z. Above $\hbar\omega \sim 35$ meV, combined resonances for the transition to the first excited subband overlap with those for the transition to the second excited subband. Above $\hbar\omega \sim 43$ meV the spectrum is very complicated because of couplings between different subbands, and we can hardly assign each peak. The position of each peak is roughly given by $E_{10}(H_y) + \Delta N\hbar\omega_c$. It is interesting that positions of small peaks are given by the same expression even for higher energies where transitions to higher excited subbands become important.

Figure 4 shows average values of z for several levels as a function of their energies in an accumulation layer. We have assumed $N_s = 1\times10^{12}$ cm^{-2}, $N_{\rm depl} = 1\times10^{8}$ cm^{-2}, $H_z = 35$ kOe, and $H_y = 20$ kOe. The Landau-level separation is 2.13 meV. The Fermi level lies in the $N = 2$ Landau level. Since the lowest two subbands are really bound states,[4] Landau series associated with them are almost unaffected in this magnetic field. The level structure for higher subbands is complicated. This figure clearly shows the complication of the accumulation case especially if we want to discuss combined resonances with positive ΔN's. Landau levels of the first excited subband already overlap with higher levels. Figure 5 gives the corresponding absorption spectrum. Even the main transitions around $\hbar\omega \sim 15.5$ meV to the first excited subband have been split because level separations of Landau levels have become different. We can see weak but distinct combined resonances $\Delta N = -1$ at $\hbar\omega \sim 12.7$ meV. There are many absorptions around $\hbar\omega \sim 17$ meV where we can expect to see combined resonances $\Delta N = +1$, and we can hardly identify them although the total absorption has a small peak at the expected position. Large absorptions at $\hbar\omega \sim 18$ meV be regarded as main transitions to the second excited subband, which have become distinct because of a nonzero H_y.

Figure 6 shows examples of calculated absorption spectra at $N_s = 1\times10^{12}$ cm^{-2}, $N_{\rm depl} = 1\times10^{8}$ cm^{-2}, and $H_z = 35$ kOe for different values of H_y. With increasing H_y the position of the weak combined resonance $\Delta N = -1$ is slightly shifted to the higher-energy side due to the diamagnetic level shift. The position of the main resonance is not shifted up to $H_y \sim 60$ kOe, which is because the diamagnetic shift is nearly cancelled by the decrease of the depolarization effect caused by the decrease of the amplitude. At $H_y \sim 50$ kOe the combined resonance $\Delta N = +1$ seems to split into two peaks. This is considered to be due to the fact that the combined resonance $\Delta N = +1$ to the first excited subband and that $\Delta N = -1$ to the second excited subband are nearly degenerate and that this degeneracy is lifted at higher H_y. Above $H_y \sim 70$ kOe the amplitude of the main resonance becomes smaller than the combined resonances and different peaks are spaced almost equally at about $\hbar\omega_c$.

Figure 7 gives positions of the various peaks as a function of N_s at $H_y = 50$ kOe and $H_z = 35$ kOe together with the subband energy separation E_{10}, $E_{10} \pm \hbar\omega_c$, and the resonance energy $\tilde{E}_{10}$ in the

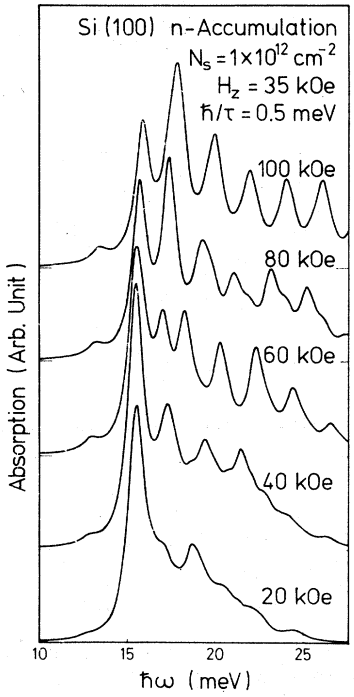

FIG. 6. Calculated optical spectra for different values of H_y in an n-channel accumulation layer on the Si (100) surface. $N_s = 1\times10^{12}$ cm^{-2} and H_z = 35 kOe. The numbers appearing in the figure represent values of H_y.

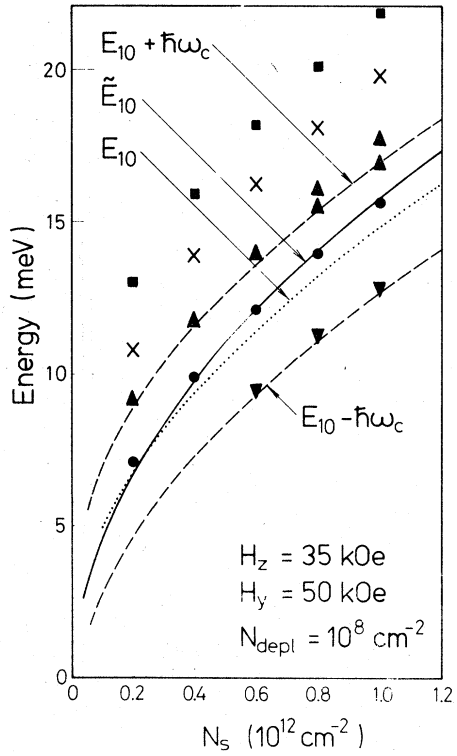

FIG. 7. Calculated positions of various peaks appearing in the optical spectra in n-channel accumulation layers on the Si (100) surface in a tilted magnetic field. H_z = 35 kOe and H_y = 50 kOe. The thin solid line represents the resonance energy for the transition from the ground to the first excited subband in the absence of a magnetic field, and the dotted line the corresponding subband energy separation. Expected positions of combined resonances for $\Delta N = \pm1$ are given by dashed lines. ●, the position of the main transition to the first excited subband; ▼, corresponding combined resonance $\Delta N = -1$. ▲, positions of the peak which consists of the combined resonances $\Delta N = +1$ to the first excited $\Delta N = -1$ to the second excited subband; ×, position of the peak regarded as the main resonance to the second excited subband; ■, position of the combined resonance $\Delta N = +1$ to the second excited subband.

absence of a magnetic field. The main resonance positions are close to $\tilde{E}_{10}$ and those of combined resonances $\Delta N = \pm1$ are close to $E_{10} \pm \hbar\omega_c$. Further we see the splitting of the combined resonance $\Delta N = +1$ above $N_s \sim 0.7\times10^{12}$ cm^{-2}. We can conclude that the observation of the combined resonances gives direct information on the strength of the depolarization effect despite the complicated level structure in the accumulation layer.

Recently such combined resonances were observed by Beinvogl and Koch in an accumulation layer.[30] An example of their results is given in Fig. 8. The absorption derivative dP/dN_s is plotted as a function of N_s for a fixed $\hbar\omega = 15.8$ meV. Roughly speaking large N_s corresponds to small $\hbar\omega$ and vice versa. The top curve corresponding to $H_y = 0$ is very close to a line shape in the absence of a magnetic field, which seems to indicate that effect of H_z are not so strong and partly justifies the assumption in the present calculation. With increasing H_y many structures appear. A structure at $N_s \sim 1.05\times10^{12}$ cm^{-2} is regarded as a combined resonance $\Delta N = +1$ and a weak structure at $N_s \sim 1.7\times10^{12}$ cm^{-2} corresponds to $\Delta N = -1$. The relative shift of the position of the main resonance from positions of the combined resonances shows the existence of the depolarization effect (positive γ_{11}) clearly.

Figure 9 gives experimental positions of the main and combined transitions in $H_z = 35$ kOe and 50 kOe for sufficiently small H_y, together with calculated E_{10}, $E_{10} \pm \hbar\omega_c$, and $\tilde{E}_{10}$, where E_{10} and $\tilde{E}_{10}$ are the subband energy separation and resonance energy in the absence of a magnetic field. First we should note that theoretical results of the resonance energy in the absence of a magnetic field are about 10% higher than the experiments. This slight difference is completely reasonable and the theoretical result is considered to be in agreement with the experiments, if we consider the simplified nature of the present model and

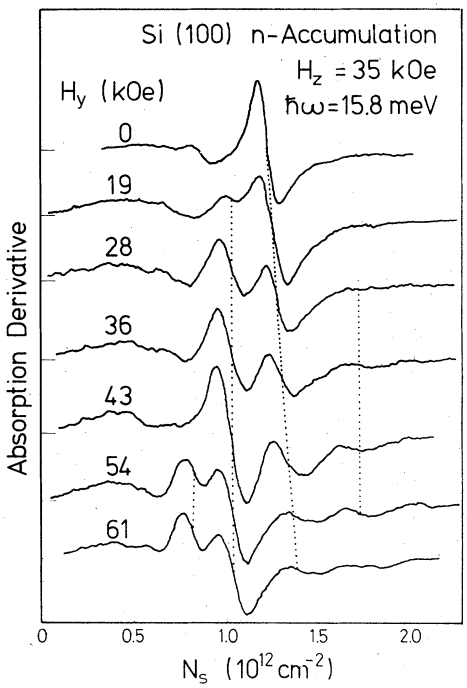

FIG. 8. Example of experimental results of Beinvogl and Koch (Ref. 30) in n-channel accumulation layers on the Si (100) surface. The absorption derivatives dP/dN_s are plotted as a function of N_s for $\hbar\omega = 15.8$ meV. The main transition is at $N_s \sim 1.2\times 10^{12}$ cm^{-2}. We can see at $N_s \sim 1.05\times 10^{12}$ cm^{-2} a combined resonance for $\Delta N = +1$, which splits into two above $H_y \sim 50$ kOe, and at $N_s \sim 1.7\times 10^{12}$ cm^{-2} a weak combined resonance for $\Delta N = -1$.

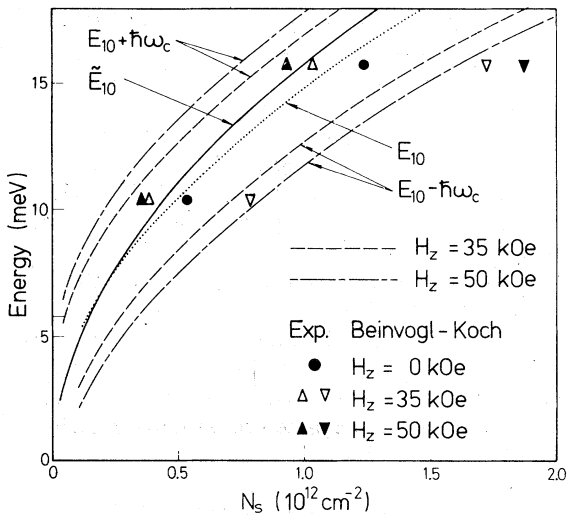

FIG. 9. Comparison of the theoretical and experimental positions of the main and the combined transitions ($\Delta N = \pm 1$) in n-channel accumulation layers on the Si (100) surface in tilted magnetic fields. $H_z = 35$ and 50 kOe. The solid line represents the calculated resonance energy and the dotted line the subband energy separation for the transition from the ground to the first excited subband in the absence of a magnetic field. Expected positions of combined resonances are given by dashed and dot-dashed lines.

approximations. A possible error might also exist on the experimental side because of uncertainties in determining exact values of N_s. The agreement is good concerning positions of the combined resonances relative to the main resonances, which shows that the theoretical result on the strength of the depolarization effect agrees with the experiments. Therefore, we can conclude that calculated subband energy separations and resonance energies are both in reasonable agreement with the experiments.

The experiments show that the combined resonance corresponding to $\Delta N = +1$ splits into two peaks above $H_y \sim 50$ kOe. This is qualitatively explained by the theory (Figs. 6 and 7), although the theoretical splitting seems to be smaller. There are a few disagreements between the theory and experiments. As is shown in Figs. 5 and 6, the theory predicts the appearance of a distinct transition to the second excited subband in nonzero H_y. Experimentally, however, such strong transition does not seem to have been observed, although we cannot give a definite conclusion because of experimental uncertainty of the absorption at low electron concentrations. The second excited subband is already a quasicontinuum state and its nature might be quite different from the ground and the first excited subband which are both bound states. The present numerical method might not describe the higher subbands well. Further electron-electron scattering effects might become important for transitions with high energies, although the effect on the transition to the first excited subband seems to be negligible since the width is related to but much smaller than the corresponding width of cyclotron resonances.[21,31]

The theory shows that the amplitude of the combined resonances become comparable to that of the main resonance around $H_y \sim 70$ kOe, while Fig. 8 shows that this occurs around $H_y \simeq 35$ kOe experimentally. Since this relative change of the amplitude is a strong function of Δ_{10}, i.e., $z_{11} - z_{00}$, this disagreement suggests that calculated extent of wave functions especially of the first excited subband is slightly too small and that it is more weakly bound in actual accumulation layers. Both experimentally and theoretically the position of the main transition is shifted to lower energies relative to the combined resonances with increasing H_y. However, experimentally positions of the combined transitions remain constant, while theoretically the position of the main transition is al-

most independent of H_y up to $H_y \sim 60$ kOe and combined resonances are shifted to higher energies due to the diamagnetic level shift. Thus the experiments do not seem to show the diamagnetic shift at all, which cannot be explained by the similar argument of the binding length and might suggest change of many-body effects in the presence of a strong magnetic field parallel and perpendicular to the surface.

From the present calculation it is clear that the accumulation layer is not the best system to study magnetic field effects because of the complicated level structure in tilted magnetic fields. Inversion layers might be much simpler and study of magnetic field effect is expected to be more fruitful. Such experiments are highly desirable.

IV. SUMMARY AND CONCLUSION

We have calculated the subband structure and the intersubband optical absorption spectrum in n-channel inversion and accumulation layers on the Si (100) surface in tilted magnetic fields, using an approximation scheme based on the density-functional theory. Effects of magnetic fields on the exchange-correlation potential have been neglected. In tilted magnetic fields combined intersubband-cyclotron transitions (transitions between different Landau levels associated with the initial and final subbands) are allowed because of coupling of electron motions parallel and perpendicular to the surface. When amplitudes of the combined resonances are sufficiently small, their positions are almost unaffected by the depolarization effect, while the main resonance is fully influenced and shifted from the subband energy separation. This is even true of accumulation layers. The results explain various features of recent experiments of Beinvogl and Koch in accumulation layers. The calculated position of the combined resonances relative to that of the main resonance is in good agreement with the experiments. Thus we can draw an important conclusion that calculated subband energy separations and resonance energies are both in reasonable agreement with the experiments. There remain some disagreements especially concerning amplitudes of the combined resonances and magnetic field dependence of their positions, which suggests slight insufficiencies of calculated wave functions and importance of effects of magnetic fields on many-body effects. Since the tilted-field effect is a very accurate test of the theory and the theory does not contain any adjustable parameters, one can conclude that it explains experiments quite well.

ACKNOWLEDGMENTS

I thank Professor J. F. Koch and Dr. W. Beinvogl for sending me their experimental results prior to the publication, and Dr. Frank Stern for critical reading of the manuscript.

---

*Present address: Institute of Applied Physics, University of Tsukuba, Sakura, Ibaraki 300-31, Japan.

[1]F. Stern and W. E. Howard, Phys. Rev. 163, 816 (1967).
[2]See, for example, T. Ando, Surf. Sci. 73, 1 (1978), and references therein.
[3]F. Stern, Jpn. J. Appl. Phys. Suppl. 2, Part 2, 323 (1974).
[4]T. Ando, Phys. Rev. B 13, 3468 (1976); Surf. Sci. 58, 128 (1976).
[5]B. Vinter, Phys. Rev. B 13, 4447 (1976); 15, 3947 (1977).
[6]F. J. Ohkawa, J. Phys. Soc. Jpn. 41, 122 (1976).
[7]P. Kneschaurek, A. Kamgar, and J. F. Koch, Phys. Rev. B 14, 1610 (1976).
[8]R. G. Wheeler and H. S. Goldberg, IEEE Trans. Electron. Dev. 22, 1001 (1975).
[9]E. Gornik and D. C. Tsui, Phys. Rev. Lett. 37, 1425 (1976).
[10]W. Beinvogl and J. F. Koch, Solid State Commun. 24, 687 (1978).
[11]W. P. Chen, Y. J. Chen, and E. Burstein, Surf. Sci. 58, 263 (1976).
[12]S. J. Allen, Jr., D. C. Tsui, and B. Vinter, Solid State Commun. 20, 425 (1976).
[13]T. Ando, Solid State Commun. 21, 133 (1977); Z. Phys. B 26, 263 (1977).
[14]T. Ando, Solid State Commun. 21, 801 (1977).
[15]F. Stern, Phys. Rev. Lett. 21, 1687 (1968).
[16]Y. Uemura and Y. Matsumoto, Suppl. J. Jpn. Soc. Appl. Phys. 40, 205 (1971).
[17]T. Ando, J. Phys. Soc. Jpn. 39, 411 (1975).
[18]W. Beinvogl, A. Kamgar, and J. F. Koch, Phys. Rev. B 14, 4274 (1976).
[19]T. Ando, J. Phys. Soc. Jpn. 44, 475 (1978).
[20]T. Ando and Y. Uemura, J. Phys. Soc. Jpn. 37, 1044 (1974).
[21]T. Ando, Z. Phys. B 24, 33 (1976).
[22]C. L. Zipfel, T. R. Brown, and C. C. Grimes, Surf. Sci. 58, 283 (1976).
[23]P. Hohenberg and W. Kohn, Phys. Rev. 136, B864 (1964).
[24]W. Kohn and L. J. Sham, Phys. Rev. 140, A1133 (1965).
[25]L. J. Sham and W. Kohn, Phys. Rev. 145, 561 (1966).
[26]T. Ando, T. Eda, and M. Nakayama, Solid State Commun. 23, 751 (1977).
[27]R. Kubo, J. Phys. Soc. Jpn. 12, 570 (1957).

[28]T. Ando, J. Phys. Soc. Jpn. 44, 765 (1978).
[29]See, for example, H. Bateman, *Higher Transcendental Functions* (McGraw-Hill, New York, 1953), Vol. 2.
[30]W. Beinvogl and J. F. Koch, Phys. Rev. Lett. 40, 1736 (1978).
[31]P. Kneschaurek, Ph.D. thesis, Physik-Department (Technische Universität München, 1976).